AL/OE-TR-1996-0124

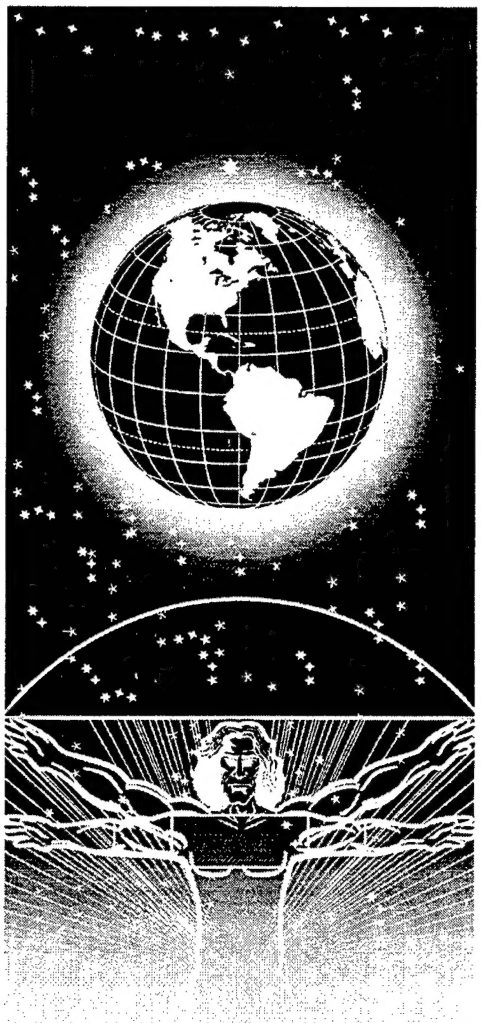

UNITED STATES AIR FORCE ARMSTRONG LABORATORY

Smoke Production And Thermal Decomposition Products From Advanced Composite Materials

D.L. Courson
C.D. Flemming
K.J. Kuhlmann
J.W. Lane

Mantech Environmental Technology, Inc.
P.O. Box 31009
Dayton, OH 45437-0009

J.H. Grabau

GEO-Centers, Inc.
7 Wells Avenue
Newton Center, MA 02159

J.M. Cline
C.R. Miller

U.S. Army Medical Research Detachment-WRAIR
2800 Q Street, Bldg. 824
Wright-Patterson AFB, OH 45433-7947

B.J. Larcom
J.C. Lipscomb

Toxicology Division
Wright-Patterson AFB, OH 45433-7400

December 1996

WRAIR-TR-95-0027

NOTICES

When US Government drawings, specifications or other data are used for any purpose other than a definitely related Government procurement operation, the Government thereby incurs no responsibility nor any obligation whatsoever, and the fact that the Government may have formulated, furnished, or in any way supplied the said drawings, specifications, or other data is not to be regarded by implication or otherwise, as in any manner licensing the holder or any other person or corporation, or conveying any rights or permission to manufacture, use, or sell any patented invention that may in any way be related thereto.

Please do not request copies of this report from the Armstrong Laboratory. Additional copies may be purchased from:

NATIONAL TECHNICAL INFORMATION SERVICE
5285 PORT ROYAL ROAD
SPRINGFIELD, VIRGINIA 22161

Federal Government agencies and their contractors registered with the Defense Technical Information Center should direct requests for copies of this report to:

DEFENSE TECHNICAL INFORMATION CENTER
8725 JOHN J. KINGMAN RD STE 0944
FT BELVOIR VA 22060-6218

DISCLAIMER

This Technical Report is published as received and has not been edited by the Technical Editing Staff of the Armstrong Laboratory.

TECHNICAL REVIEW AND APPROVAL

AL/OE-TR-1996-0124
WRAIR-TR-95-0027

The animals used in this study were handled in accordance with the principles stated in the *Guide for the Care and Use of Laboratory Animals* prepared by the Committee on Care and Use of Laboratory Animals of the Institute of Laboratory Animal Resources, National Research Council, National Academy Press, 1996, and the Animal Welfare Act of 1966, as amended.

This report has been reviewed by the Office of Public Affairs (PA) and is releasable to the National Technical Information Service (NTIS). At NTIS, it will be available to the general public, including foreign nations.

This technical report has been reviewed and is approved for publication.

FOR THE COMMANDER

TERRY A. CHILDRESS, Lt Col, USAF, BSC
Director, Toxicology Division
Armstrong Laboratory

REPORT DOCUMENTATION PAGE

Form Approved
OMB No. 0704-0188

1. AGENCY USE ONLY (Leave Blank)	2. REPORT DATE	3. REPORT TYPE AND DATES COVERED
	December 1996	Interim - January 1995 - December 1995

4. TITLE AND SUBTITLE
Smoke Production and Thermal Decomposition Products from Advanced Composite Materials

5. FUNDING NUMBERS
Contract F41624-96-C-9010
PE 62202F
PR 7757
TA 7757A1
WU 7757A103

6. AUTHOR(S)
D.L. Courson, C.D. Flemming, K.J. Kuhlmann, J.W. Lane, J.H. Grabau, J.M. Cline, C.R. Miller, B.J. Larcom, and J.C. Lipscomb

7. PERFORMING ORGANIZATION NAME(S) AND ADDRESS(ES)
ManTech/GeoCenters Joint Venture
P.O. Box 31009
Dayton, OH 45437-0009

8. PERFORMING ORGANIZATION REPORT NUMBER

9. SPONSORING/MONITORING AGENCY NAME(S) AND ADDRESS(ES)
Armstrong Laboratory, Occupational and Environmental Health Directorate
Toxicology Division, Human Systems Center
Air Force Materiel Command
Wright-Patterson AFB OH 45433-7400

10. SPONSORING;MONITORING AGENCY REPORT NUMBER
AL/OE-TR-1996-0124
WRAIR-TR-95-0027

11. SUPPLEMENTARY NOTES

12a. DISTRIBUTION/AVAILABILITY STATEMENT
Approved for public release; distribution is unlimited.

12b. DISTRIBUTION CODE

13. ABSTRACT (Maximum 200 words)

This report describes the smoke production and thermal decomposition products from the combustion of Advanced Composite Materials (ACM) used on high performance aircraft. There are three distinct project phases with only Phase I described here. The preliminary work (Phase 0) addressed the physical behavior of burning composites, such as mass loss rates, smoke plume dispersion, and the environmental impact of a burning aircraft. Results of Phase 0, characterizing and modeling emissions along with subsequent dispersion were presented in TR-AFIT/GEEM/ENV948-21 (Roop et al, 1994).

Phase I involves applying methods developed in Phase 0 to chemical and morphological characterization of the smoke produced in a small-scale wind tunnel. Results from these experiments and analytical findings are presented in this report. The combustion conditions were selected to represent a range of real-world scenarios to evaluate potential health effects from exposure to smoke and thermal decomposition products generated during burning of ACM. An analytical protocol for evaluating the characteristics of smoke produced from controlled combustion of test materials was developed. The combustion apparatus used is a modified form of the cone heater combustion module of the UPITT II method developed at the University of Pittsburgh.

Phase II is currently underway and will describe the *in vivo* effects of acute exposure to smoke from burning composition materials.

14. SUBJECT TERMS
Advance Composite Materials (ACM) Exposure Combustion

15. NUMBER OF PAGES
54

16. PRICE CODE

17. SECURITY CLASSIFICATION OF REPORT	18. SECURITY CLASSIFICATION OF THIS PAGE	19. SECURITY CLASSIFICATION OF ABSTRACT	20. LIMITATION OF ABSTRACT
UNCLASSIFIED	UNCLASSIFIED	UNCLASSIFIED	UL

NSN 7540-01-280-5500

Standard Form 298 (Rev. 2-89)
Prescribed by ANSI Std. Z39-18
298-102

THIS PAGE INTENTIONALLY LEFT BLANK

TABLE OF CONTENTS

LIST OF FIGURES

FIGURE PAGE

LIST OF TABLES

PREFACE

The research reported herein was conducted by the Tri-Service Toxicology Consortium and initiated by Dr. Daniel Caldwell as the principal investigator. Authors would like to acknowledge the technical support of Ms Merry Jane Walsh, Mr. Willie Malcomb, SPC David Peterson, Ms Lauren Silvers, and SrA Frank Dessauer.

This is a technical report describing the smoke production and thermal decomposition products from the combustion of Advanced Composite Materials (ACM) used on high performance aircraft. There are three distinct project phases with only Phase I described here. The preliminary work (Phase 0) addressed the physical behavior of burning composites, such as mass loss rates, smoke plume dispersion, and the environmental impact of a burning aircraft. Results of Phase 0, characterizing and modeling emissions along with subsequent dispersion, were presented in TR-AFIT/GEEM/ENV/94S-21 (Roop et al, 1994).

Phase I involves applying methods developed in Phase 0 to chemical and morphological characterization of the smoke produced in a small-scale wind tunnel. Results from these experiments and analytical findings are presented in this report. The combustion conditions were selected to represent a range of real-world scenarios to evaluate potential health effects from exposure to smoke and thermal decomposition products generated during burning of ACM. An analytical protocol for evaluating the characteristics of smoke produced from controlled combustion of test materials was developed. The combustion apparatus used is a modified form of the cone heater combustion module of the UPITT II method developed at the University of Pittsburgh.

Phase II is currently underway and will describe the *in vivo* effects of acute exposure to smoke from burning composite materials.

ABBREVIATIONS

ACM	Advanced Composite Materials
°C	Degrees Celsius
g	Gram
GC/MS	Gas chromatography/mass spectroscopy
L/min	Liters per minute
min	Minute
ml	Milliliter
EPA	US Environmental Protection Agency
V	Airflow (L/min)
Q	irradiance or heat flux (kW/m^2)
m^2	Meter squared
ft^2	Feet squared
ft	Feet
PID	Proportional Integral Derivative
kW/ m^2	Kilowatt/meter squared
T_{ign}	Time of Ignition
T_{fl}	Duration of flaming
m	Mass loss rate
CPVC	Chlorinated polyvinyl chloride
CO	Carbon Monoxide
CO_2	Carbon Dioxide
O_2	Oxygen
SEM	Scanning electron microscope
um	Micrograms
nm	Nanometers
KV	Kilovolts
CCD	Charged-coupled device
GLM	General Linear Model
ANOVA	Analysis of Variance
CNS	Central nervous system
PAHs	Polycyclic Aromatic Hydrocarbons
NIOSH	National Institute of Occupational Safety and Health
PPE	Personal protective equipment

THIS PAGE INTENTIONALLY LEFT BLANK

INTRODUCTION

The demand for lightweight materials of high strength and improved thermoplastic properties (rigidity, conductivity, thermal expansion) has resulted in the extensive development and application of Advanced Composite Materials (ACM). These materials generally consist of a reinforcing fiber matrix incorporated into an epoxy resin binder (Figure 1). The current use of graphite-based composites is increasing as manufacturers exploit the unique advantages of this structural material. However, their flammability characteristics and performance are significantly different from their metal counterparts. Use of new synthetic materials, such as ACM, raises concerns about the potential environmental and human health risk resulting from exposure to the chemically complex smoke produced by burning these materials. Although ACM appear to present no danger to human health in their original state, the chemical transformation of this material during combustion is not well characterized. The resins used in binder material

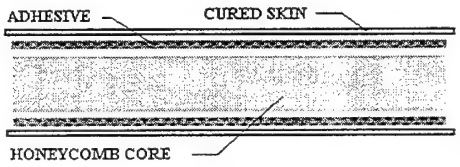

Figure 1. Typical Cross-Section of Advanced Composite Material

may release potentially harmful gases, vapors, or fibrous materials when burned. Similar situations could occur during operational conflicts for flight line personnel and crew members.

Carbon fiber composites were introduced as a substitute for fiberglass, and were found to be stronger than either fiberglass or aluminum panels. The use of carbon composites in aircraft is increasing as manufacturers learn to use the strengths of ACM. Advanced filamentary composite materials provide many advantages over metals and also offer added fatigue and corrosion resistance, controlled thermal expansion, dimension stability, and the ability to form complex-shaped parts without increasing the potential for fatigue.

Two distinct categories of matrix resins are used in advance composite: thermosets and thermoplastics. Historically, continuous fiber reinforced composite applications have been dominated by matrices consisting of thermosetting resins such as epoxies and bismaleimides (BMI). Epoxy resin polymers are known for their superior properties. These include good bonding to several substrates, good chemical resistance, and a wide availability of form to meet the requirements of the manufacturer. In addition, thermosets burn for a shorter period and char rather then soften or melt like a thermoplastic. High performance thermoplastic matrix materials provide alternatives to the thermosetting matrix composite for aerospace applications. Thermoplastic resins are stable, high molecular weight polymers that retain their chemical stability throughout

processing (no chemical reactions occurs during processing). Toughness, durability, strength, and reparability are the driving forces for adapting thermoplastics for use in advanced composites.

Military aviation mishaps have resulted in illness to fire safety personnel as a result of exposure to toxic gases from burning composite materials (Ohlemiller et al, 1993). During an aircraft mishap, the composite structures are subjected to forces that cause them to break into pieces, burn, and subsequently release aggregates or particulates to the local environment. The reinforcement fibers, which are very stiff and give the composite its strength, may be dismembered into smaller elements of varying size causing potential respiratory hazard(s).

The fire hazards of organic composites are not well understood but depend on many factors including actual conditions of use (e.g., geometry and orientation), proximity of other materials, environmental conditions, ignition sources, as well as the intrinsic properties of the composite such as chemical composition, thermal stability, and heat transfer characteristics. Expected variations in decomposition rates will substantially affect the constituency and concentrations of combustion products. Particle distribution and rate of release may also depend on local environmental conditions (Babrauskas et al, 1987). Evidence also indicates that increased smoke and toxic gas generation rates result from conventional attempts to incorporate self-extinguishing or fire retarding formulation in the matrix materials. Under conditions of sustained heat flux and great amounts of entrained air, the ACM will burn more vigorously, generating very high heat energy, smoke, and toxic gas concentrations.

Research Objectives

Primary objective of this work was to determine smoke production and atmosphere characteristics from burning ACM.

Secondary purpose of this research was to simulate an aircraft mishap by burning advanced-composite coupons and characterize the fibrous aerosol emissions.

To meet these two objectives, two research questions were posed:

Research Question 1: What is the constituents and concentration of the smoke produced vapor and particulate during combustion of ACM with simulated 5, 10 and 15 mile per hour winds?

Research Question 2: How can the smoke and aerosol plume generated during thermal decomposition of ACM material be accurately characterized?

Research Hypothesis: A modified UPITT II can be used to adequately generate the aerosol plume produced from burning ACM.

Scope and Limitation: Smoke generated during the combustion of most materials is very complex and generally toxic (Caldwell and Alarie, 1990). The absorption of thermal decomposition products onto soot released from burning ACM could facilitate the movement of these products into the lung and increase their retention, thus exacerbating the toxic effects. Evaluating the toxicity of carbon and graphite fibers is beyond the scope of this report and will be addressed in the follow-on phase three effort. Any speculation on environmental effects is beyond the scope of this project.

MATERIALS AND METHODS

Materials

A carbon fiber/modified bismaleimide resin ACM (approximate 2:1 ratio by weight) was used in these studies. Specimens were 108 mm square by 2.5 mm thick with a mass of 53.90 $\pm$ 0.36 g.

Preliminary Investigation

A modified UPITT II cone calorimeter (Fire Testing Technology Inc.) was utilized in the collection of ACM combusted material for initial analysis (Figure 2). Two samples of combustion products were collected and analyzed in a Perkin-Elmer 910 GC/MS (Gas Chromatograph/Mass Spectrometer) system (see Appendix A for GC/MS conditions). The first sample was a portion (vapor) of the smoke plume caught in a cold trap, extracted with methylene chloride, and concentrated with a stream of dry nitrogen. The cold trap consisted of a glass impinger in an ice/water bath connected to the end of the calorimeter train. A total of 150 liters (10 L/min for 15 min) of the combustion gas was drawn through the trap. The second sample of deposited soot was collected on a glass wool filter. Soot is defined as a fine particulate material created during combustion and deposited throughout the apparatus. The standard method for extraction (Soxhlet) could not be employed due to the particle size. Instead, a glass pipette plugged with glass wool was used. The apparatus was cleaned with 50:50 methylene chloride:acetone, the soot added, and the same solvent mix was passed through the soot until no more color was noticed in the solvent as it drained from the pipette. The extract was concentrated to approximately 1 ml by a stream of dry nitrogen and then made up to 20 ml with methylene chloride.

Compound identification was performed quantitatively using the latest available NIST reference library and approximate quantification was performed under EPA Method 8270 protocols. Identification was conducted as a qualitative assessment for preliminary investigation.

Figure #2

Combustion System #1

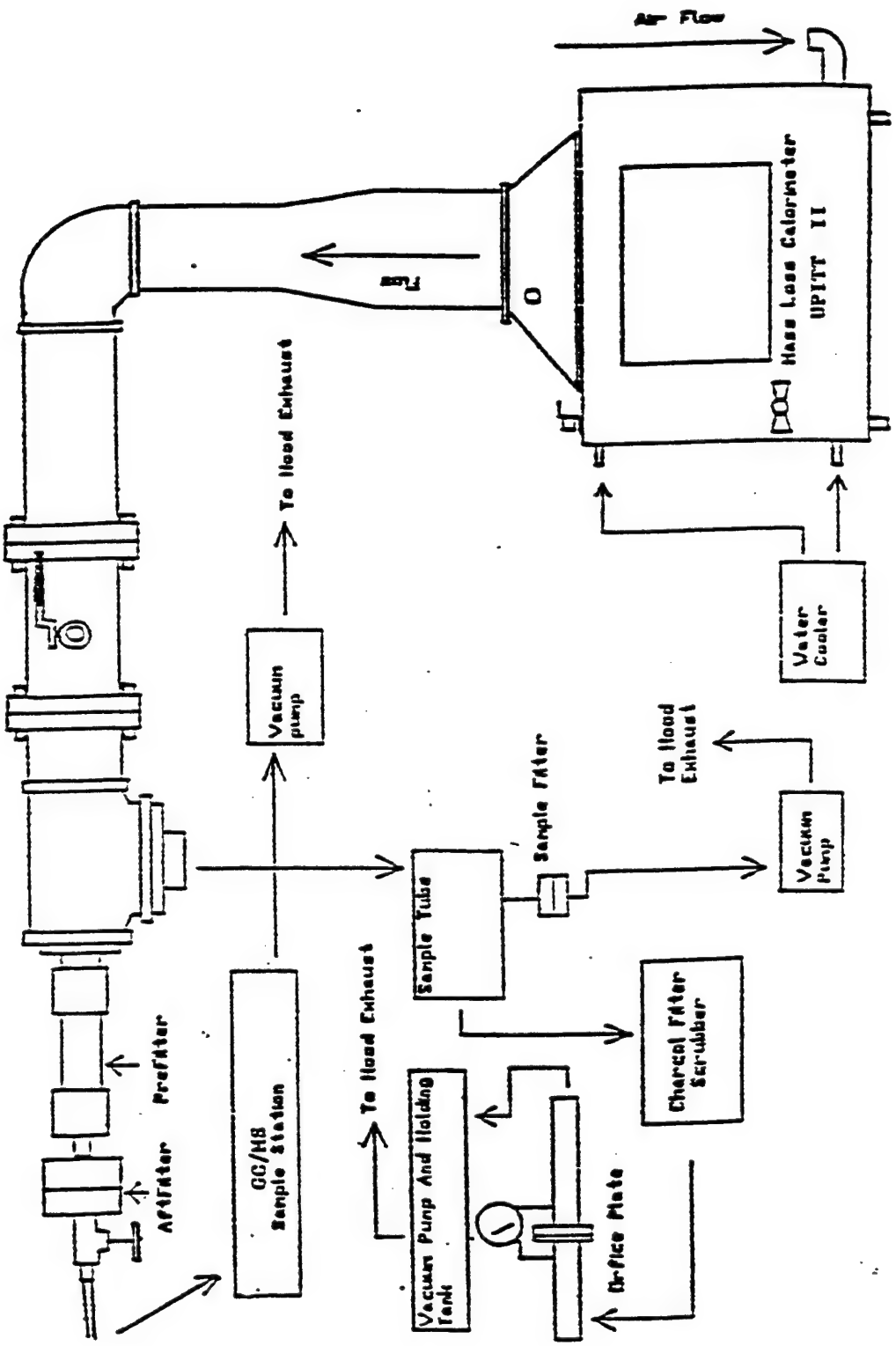

Combustion Apparatus & Tunnel Design (Figure 3)

A protocol to evaluate the combustion products of ACM was developed using a modified UPITT II method, which permits control of heat flux, (Q), and airflow, (V), the fundamental variables determining combustion conditions, and simultaneously measures mass loss rate (Caldwell et. al. 1990a and Miller et. al. 1995). A mini-cone calorimeter, similar to that used in the UPITT II combustion apparatus, was used to simulate real world exposure scenarios with experimentally controlled combustion conditions. The mini cone calorimeter (Fire Testing Technology Inc.) consisting of a truncated cone-shaped heating element which was used to irradiate the ACM sample (approximately 0.01 m^2 ACM "coupon") at selected heat flux levels. A load cell was incorporated into the sample platform, allowing approximate measurement of mass loss during controlled combustion. The entire apparatus was contained in a ventilated 16 ft^2 plexiglas containment unit. A Proportional Integral Derivative (PID) device (Eurotherm) controlled the temperature of the cone calorimeter and was positioned on top of the containment unit. Airflow through the system was maintained by pulling air (unfiltered) through the cone calorimeter and sampling train. Smoke exited the UPITT II via a 3 inch stainless steel tube which was immediately reduced to 2.5 inch. The 2.5 inch tube incorporated a 90° bend and was flanged to an apparatus utilized for collection of gas samples (not shown in figure 3). Main body of flow continued into a 12.5 inch diameter CPVC duct 40 ft in length. Five sampling ports were installed at 10 ft intervals along the length of the tunnel to allow for direct sampling of the smoke plume (Figure 4). Stainless steel tubes ran from the sampling port to the center of the tunnel and were bent 90° into the air stream. Access ports (6 inch holes) were drilled into the tunnel and sealed with removable plugs for ready access to the sampling devices inside the tunnel. Exhaust from the tunnel was pulled through a high efficiency particulate air filter and mist air scrubber and vented into a laboratory hood.

Twenty smoke tests were conducted as part of a cross-classified design of three levels of Q, 38.5, 57.2, and 84.2 kilowatts per square meter (kW/m^2) corresponding to 625°, 770°, and 880°C, and four levels of V, 340, 370, 400, and 650 liters per minute (L/min). Thermocouples were placed at 10 ft intervals (sampling ports) along the tunnel and positioned in the center of the air stream to continuously monitor temperature. The time to ignition (T_{ign}), duration of flaming (T_{FI}), and mass loss rate (m) over a 10 minute period were determined as described in Caldwell et. al. 1990b, 1991, 1995.

Combustion Product Identification

Gas monitoring instruments (Rosemount Industries) sampling the smoke plume in the section between the cone calorimeter and the 12.5 inch CPVC duct provided continuous monitoring of carbon monoxide (CO), carbon dioxide (CO_2), and oxygen (O_2) concentrations during experiments. The digital output from these analyzers was collected in real time and stored on a computer equipped with a 1601 Keithley-Metrabyte data acquisition card.

Figure #1

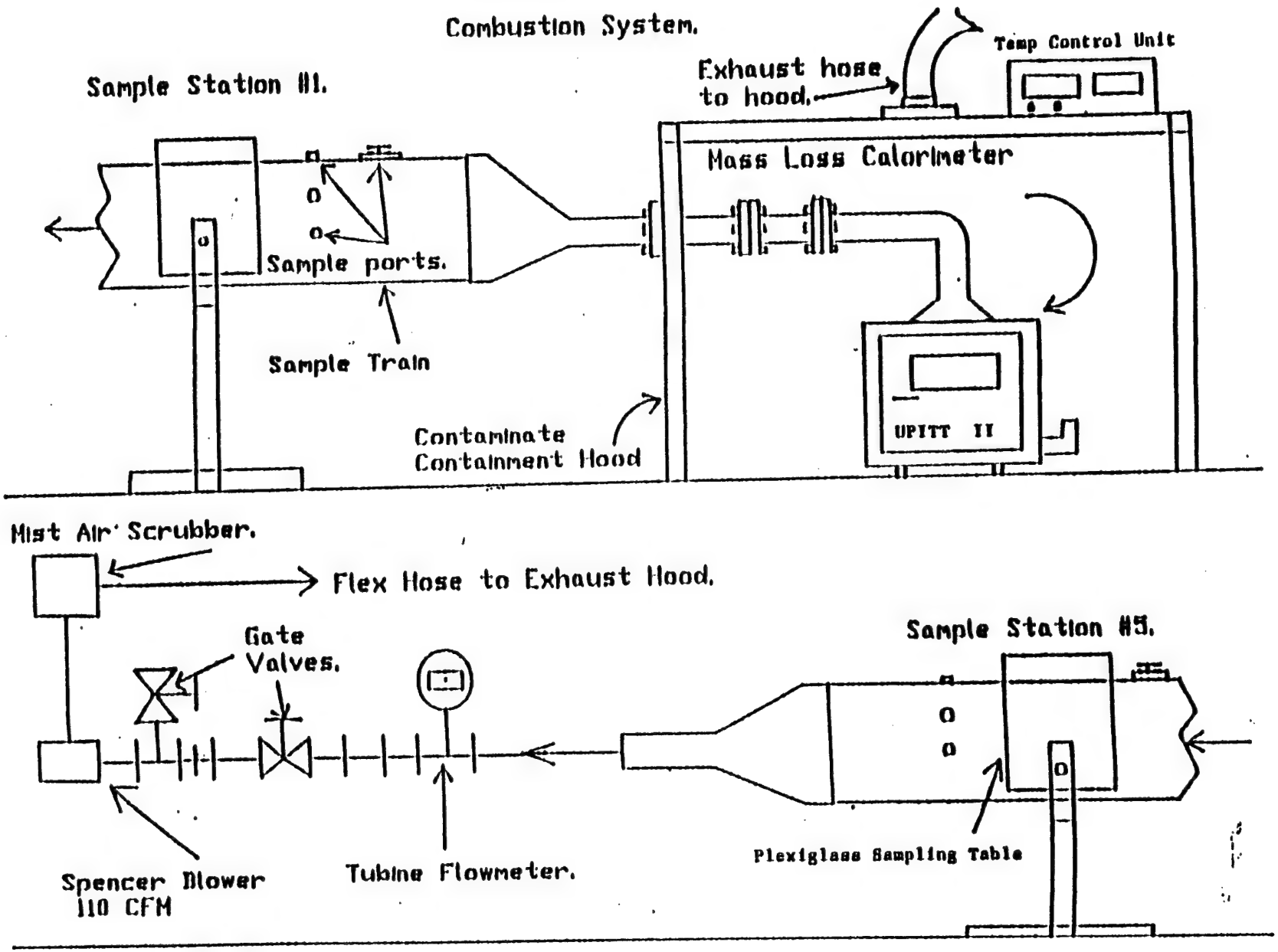
Combustion System.
Temp Control Unit
Exhaust hose to hood.
Sample Station #1.
Mass Loss Calorimeter
Sample ports.
Sample Train
Contaminate Containment Hood
UPITT II
Mist Air Scrubber.
Flex Hose to Exhaust Hood.
Gate Valves.
Sample Station #5.
Spencer Blower 110 CFM
Tubine Flowmeter.
Plexiglass Sampling Table

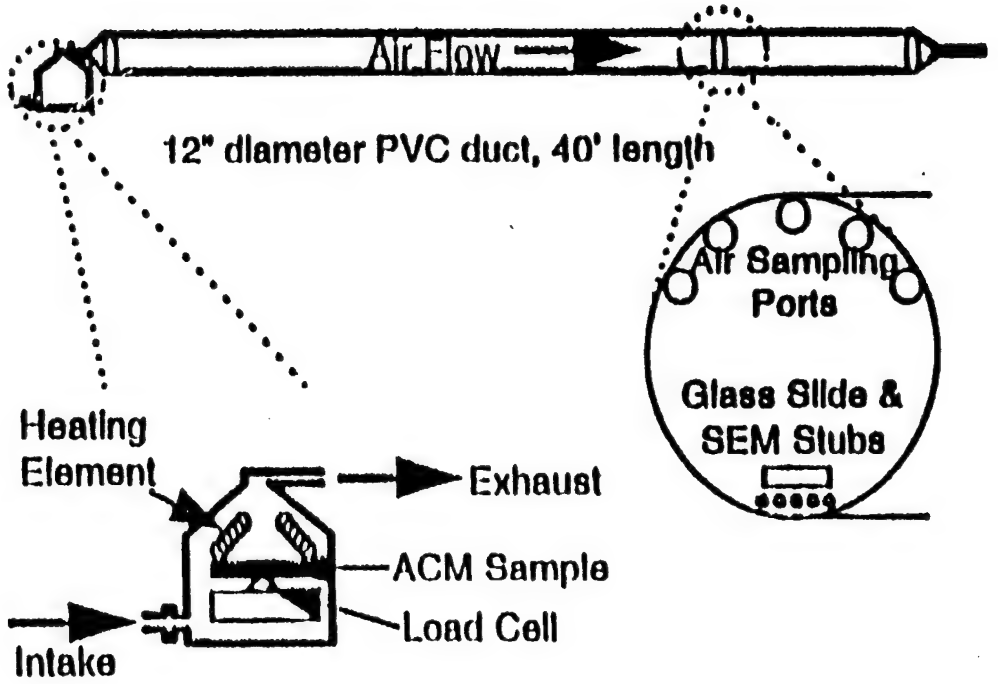

Figure 1. Tunnel Diagram.

Several sampling techniques were investigated and tested for the collection of smoke products generated during combustion: (a) multi-stage cascade impactors, (b) single stage impactors, (c) polycarbonate air filters, (d) electrostatic precipitation, (e) miniature cyclone deposition, and (f) gravitational settling of particles from the air stream onto aluminum scanning electron microscope (SEM) stubs and glass microscope slides placed on the bottom of the tunnel.

A multi-jet, multi-stage cascade impactor fitted with a glass fiber filter in the final stage was used to determine the aerodynamic diameter of the aerosol particles. Because the smoke concentration was quite high close to the combustion chamber, trials showed that sampling devices located along the first section of the tunnel would rapidly become overloaded. Therefore, a cyclone separator (In-Tox Products) was connected in series with the first multi-stage cascade impactor (located at section number one) to remove particles greater than 10 um from the sampling stream, preventing overloading of the impactor. Gilian Aircon-2 High Flow sampling pumps calibrated to 20 L/min were used with the impactors; exhaust gas from the pump was routed back into the tunnel downstream of the sampling port with tygon tubing. Cleaned aluminum SEM stubs prepared with an adhesive substrate were placed in a stainless steel holder and positioned on the bottom of the tunnel at 10 ft intervals. Holders were positioned parallel to the airstream and slightly upwind of the access ports so that removal of the plug at the end of each run would not knock material onto the sampling surface. Glass microscope slides placed adjacent to the SEM stubs were also used as a collection surface for aerosol particles. Modeling clay formed into low-profile holders with recesses for 2 slides was set in the bottom of the tunnel upwind of the SEM stubs. A point-to-plane electrostatic precipitator (In-Tox Products) was connected to the tunnel at section number one. This instrument was configured to collect aerosol particles onto polished carbon SEM planchettes.

Particulate samples for evaluation by SEM were dried overnight in a vacuum desiccator, then sputter-coated with a 10-15 nm layer of gold. Photomicrographs were taken of the surfaces using an Amray 1000B SEM at 20-30 kV accelerating voltage.

Algorithms developed for particle analysis were employed using a Quantimet 570c image analysis system (Leica, Inc). Samples collected on glass microscope slides were magnified to 40x, 200x and 400x on a light microscope and the resulting images captured by a microscope-mounted CCD camera and digitized for image analysis. Photographs obtained by SEM were captured by a CCD camera mounted on a macro-(photo)stand. Particles were detected as "features" in each calibrated digitized image by comparing the gray level of the feature with the background gray level. The identified features were then measured using computer-based image analysis methodologies for area, perimeter and equivalent circle diameter.

Statistical Analyses

Two General Linear Model (GLM) one-factor analysis of variance (ANOVA) were used to determine the effect of temperature and the effect of flow rate on mass loss. The Shapiro-Wilk statistic was used to test the normality of the data (Shapiro, 1961; Royston, 1982). The equality of variances among the temperatures and among the flow rates was done using Levene's test of equal variances (Levene 1960). Since most of the twenty smoke tests were unreplicated, a two-factor ANOVA using the two-way (temperature X flow rate) interaction term as an error term was used to determine the effects of temperature and flow rate on gas (CO, CO_2, O_2) levels (Winer, 1971). Multiple comparisons were done using Bonferroni adjustments (Hochberg, 1987). A three-way contingency table analysis was used to analyze particulates since some of the larger particles influenced the mean. The three-way interaction was significant among temperature, flow rate, and interval thus, a two-way interaction between temperature and interval was done for each flow rate, and a two-way interaction between flow rate and interval was done for each temperature. The distribution was a chi-squared.

RESULTS

Preliminary Investigation

Numerous organic compounds were tentatively identified by extraction from the soot (Appendix B). The major compounds based on percent weight of the soot at the collection site are listed in Table 1.

TABLE 1. IDENTIFICATION AND APPROXIMATE QUANTITATION OF MAJOR COMPOUNDS EXTRACTED FROM SOOT

Identified Compound	Concentration in Soot (μg/g)	Concentration in Soot (% Weight)
Aniline	2990	0.30%
Phenol	2170	0.22%
2- and 3-Methylaniline	1200	0.12%
Quinoline	3480	0.35%
5-Methyquinoline	1200	0.12%
Diphenylether	1050	0.11%
2-Methoxyethoxybenzene	1660	0.17%
1,2-Dihydro-2,2,4-trimethylquinoline	2210	0.22%
2-Isocyanonaphthalene	2210	0.22%
Dibenzofuran	1360	0.14%
1-Isocyanonaphthalene	1660	0.17%
Anthracene	1700	0.17%
N-Hydroxymethylcarbazole	1290	0.13%
Fluoranthene	2130	0.21%

Eight chemicals, four of which are also in the soot, were identified in the representative vapor sample (Table 2).

TABLE 2. APPROXIMATE CONCENTRATIONS OF VAPOR COMPOUNDS

Compound	Air Conc. (ug/m3)
Aniline	571
Phenol	1600
4-methylphenol	106
2-methylphenol	125
3-isocynatotoluene	9.8
Quinoline	41.5
Biphenyl	11.4
Diphenyl Ether	190

During the analytical process it was apparent upon examination of the injection port liner that many of the extracted compounds were not suitable for analysis by GC/MS, due to pyrolysis and deposition in the liner. There were a number of Polycyclic Aromatic Hydrocarbon (PAH) peaks in the soot extract which were of too low in strength to characterize properly, and were not included in the above. There are probably a considerable number of compounds which either did not extract or did not make it out of the GC injection port.

Mass Loss

The data was normally distributed ($w=0.9297$, $p=0.2660$) and variance among flow rates ($p=0.8828$) and temperature ($p=0.344$) were equal. The mass loss rate was found to increase from 625°C to 770°C ($p=0.0512$). The greatest mass loss occurred at 770°C and the least at 880°C ($p=0.0098$), however there was no statistical difference between 625°C and 880°C ($p=0.5940$). See Figure 5. There was no significant difference among flow rates ($p=0.5622$) but an effect was noted due to temperature variation ($p=0.0094$). Table 3 identifies the burn parameters, mass loss and flame conditions.

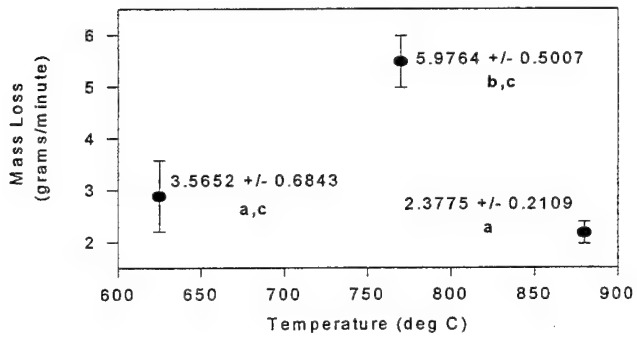

Figure 5. ACM Coupon Mass Loss Rate at Three Temperatures.

TABLE 3. SPECIMEN MASS, MASS LOST, TIME OF SMOKE/IGNITION/FLAME, DURATION OF FLAME, AND MASS LOSS RATE DURING FLAMING AND OVER A 10 MINUTE PERIOD AT INDICATED BURNING CONDITIONS

Burn ID	Temp	Airflow	ACM Mass	Mass Lost	Mass Lost	Smoke	Time of: Ignition	Flame	Flame duration	m Tflame	m 10 min
	°C	(L/min)	(g)	(g)	%	(mm:ss)	(mm:ss	(mm:ss	(min)	(g/min)	(g/min)
b	625	340	53.90	9.94	18.4	00:08	00:33	05:40	5.12	1.941	0.994
c	625	340	54.20	11.46	21.1	02:00	02:30	06:34	4.06	2.823	1.146
e	625	340	58.95	15.04	25.5	01:42	02:06	05:32	3.43	4.385	1.504
f	625	340	59.12	15.59	26.4	01:20	01:35	07:00	5.42	2.876	1.559
h	625	370	60.69	14.93	24.6	01:39	02:17	06:08	3.85	3.878	1.493
i (!!)	625	400	60.39	10.12	16.8	01:41	01:45	---	---	---	1.012
i2	625	400	60.03	14.95	24.9	01:42	02:00	06:15	4.25	3.518	1.495
k	625	650	60.13	15.69	26.1	01:31	01:47	04:03	2.27	6.912	1.569
j (@)	770	400	60.52	19.80	32.7	00:27	00:28	03:26	2.97	6.667	1.98
l (#)	770	650	59.99	19.34	32.2	00:30	00:42	04:09	3.45	5.606	1.934
l2	770	650	58.93	17.41	29.5	00:30	01:10	04:38	3.47	5.017	1.741
s	770	340	60.50	20.05	33.1	00:31	00:46	04:16	3.50	5.729	2.005
t ($)	770	370	59.36	18.10	30.5	00:06	00:07	02:34	2.45	7.388	1.81
m	880	650	59.02	22.26	37.7	00:08	00:14	10:00	9.77	2.278	2.226
o	880	340	59.04	21.23	36	00:17	00:18	10:00	9.70	2.189	2.123
p	880	370	60.43	19.86	32.9	00:09	00:27	07:05	6.52	3.046	1.986
q	880	400	59.54	19.32	32.4	00:17	00:34	10:00	9.43	2.049	1.932

Notes: !! flame died immediately after igniter was removed
@ shutter left open during sample loading and temperature ramp-up
# filter to gas analyzer incorrectly installed, restricting flow to analyzers
$ sample held at temperature for 5 min prior to opening shutter

Gas Analysis

There were no significant differences among the temperatures for the maximum value of CO ($p = 0.2104$), for the maximum value of CO_2 ($p = 0.2780$) and for the minimum value of O_2 ($p = 0.2811$). Among the temperatures, the data was statistically normal, and the data showed equal variances (Table 4).

There were no significant differences among flow rates for the maximum value of CO ($p = 0.0910$). However, there were significant differences for the maximum value of CO_2 ($p = 0.0083$) and for the minimum value of O_2 ($p = 0.0017$), see Table 4. Among the flow rates, all of the data was normally distributed and had equal variances. The maximum CO_2 value decreased and the minimum O_2 value increased as flow rate increased. Figures 6-14 graphically demonstrate each temperature at the various flows for each gas.

TABLE 4. AVERAGE PERCENTAGES (± STANDARD ERROR) OF CARBON MONOXIDE (CO), CARBON DIOXIDE (CO_2), AND OXYGEN (O_2) FOR THE DIFFERENT BURN TEMPERATURES (n = 4) AND FOR THE DIFFERENT FLOW RATES (n = 3)

Temperature (°C)	CO % (max) (p= 0.2104)	CO_2 % (max) (p= 0.2780)	O_2 % (max) (p= 0.2811)
625	0.137 ± 0.024	2.42 ± 0.287	18.01 ± 0.491
770	0.251 ± 0.191	3.11 ± 0.653	17.31 ± 0.809
880	0.283 ± 0.083	2.74 ± 0.655	17.69 ± 0.870

Flow Rate (L/min)	CO % (max) (p= 0.0910)	CO_2 % (max) (p= 0.0083)	O_2 (max) (p= 0.0017)
340	0.373 ± 0.094	4.17 ± 0.487	15.68 ± 0.509
370	0.179 ± 0.015	2.60 ± 0.18*	17.83 ± 0.195
400	0.243 ± 0.101	2.54 ± 0.415*	18.14 ± 0.41
650	0.100 ± 0.007	1.72 ± 0.13	19.02 ± 0.088

* not significantly different from one another

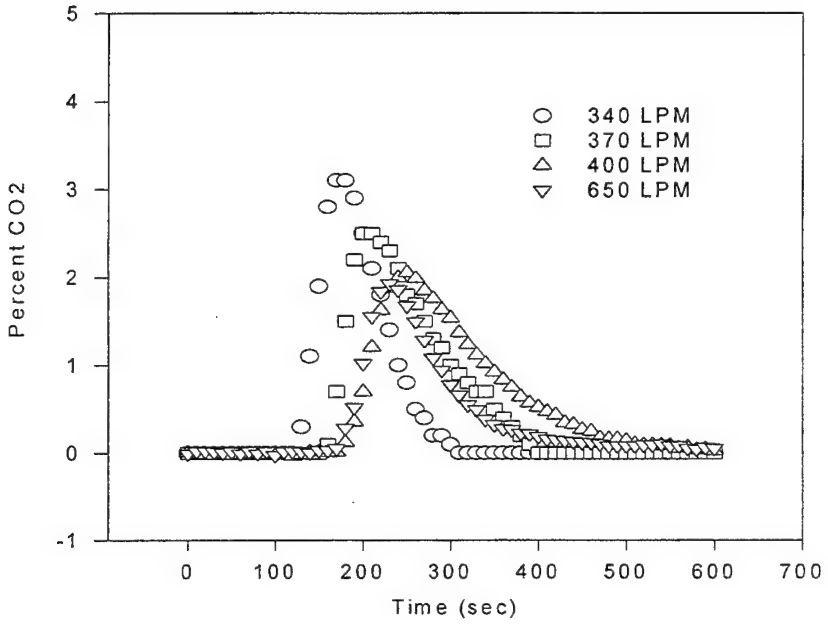

Figure 6. Carbon Dioxide production at 625 degrees C.

At 625 degrees, the maximal concentration of carbon dioxide is reached at approximately 160 seconds at the lowest flow rate. Increasing the flow rate diminishes the maximal observed concentration of carbon dioxide and prolongs the time required to reach maximal concentration.

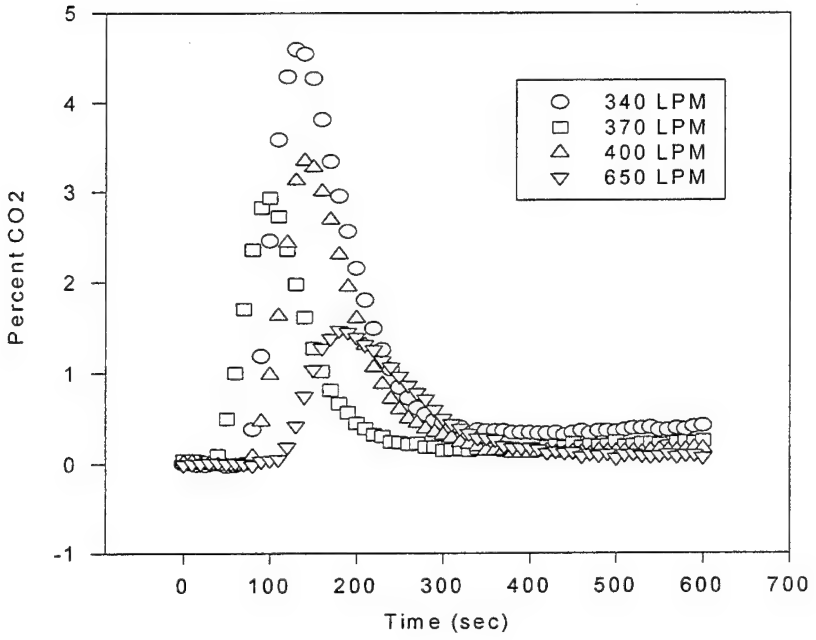

Figure 7. Carbon Dioxide production at 770 degrees C.

At 770 degrees, the maximal carbon dioxide concentration is reached at approximately 110 seconds. An increase in flow rate from 340 LPM to 370 LPM resulted in a decrease in the time-to-peak. Further increases in flow decreased the maximal observed concentration and lengthened the time to maximal concentration.

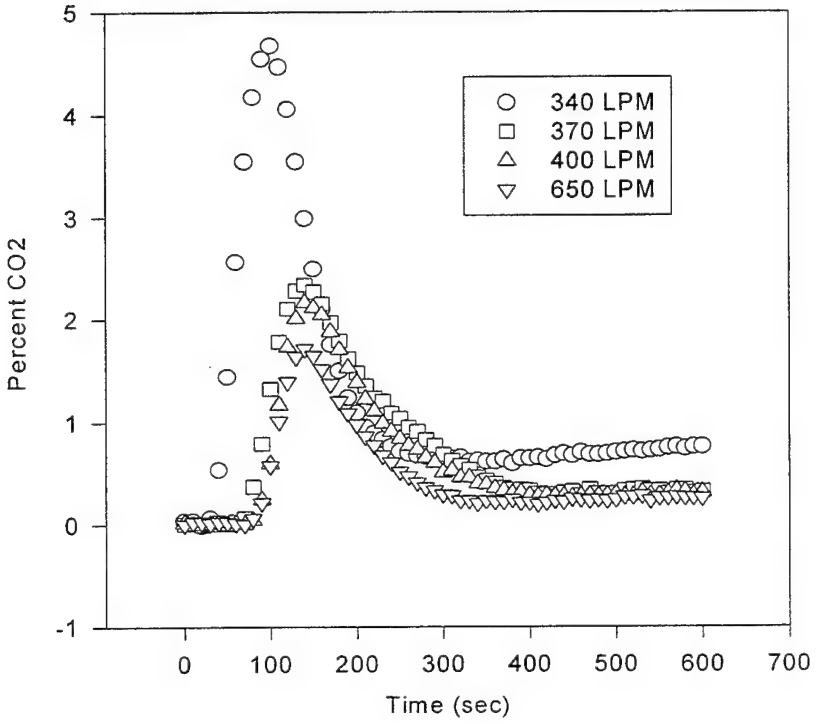

Figure 8. Carbon Dioxide production at 880 degrees C.

At 880 degrees, the maximal carbon dioxide concentration is reached at approximately 90 seconds and is highest at the 340 LPM (lowest) flow rate. Increases in flow rate result in decreased maximal observed concentrations and increased time required to reach maximal concentrations.

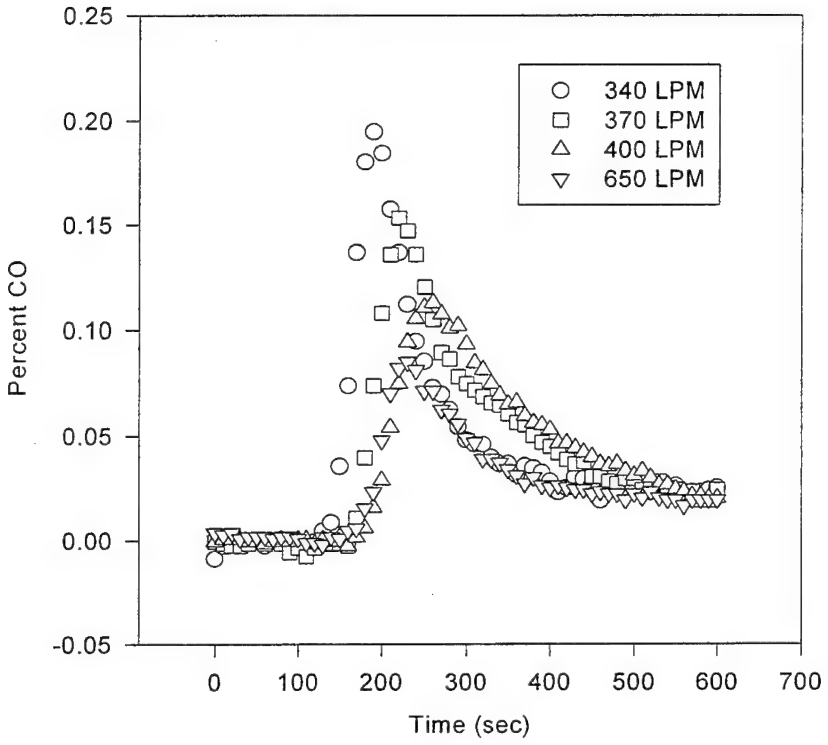

Figure 9. Carbon Monoxide production at 625 degrees C.

Carbon monoxide maximal concentrations were observed at approximately 175 seconds when evaluated at burn temperature of 625 degrees. The maximal observed concentration is much lower than the maximal concentration observed at higher temperatures. Increasing the flow rate results in decreased maximal concentration and increased time-to-peak.

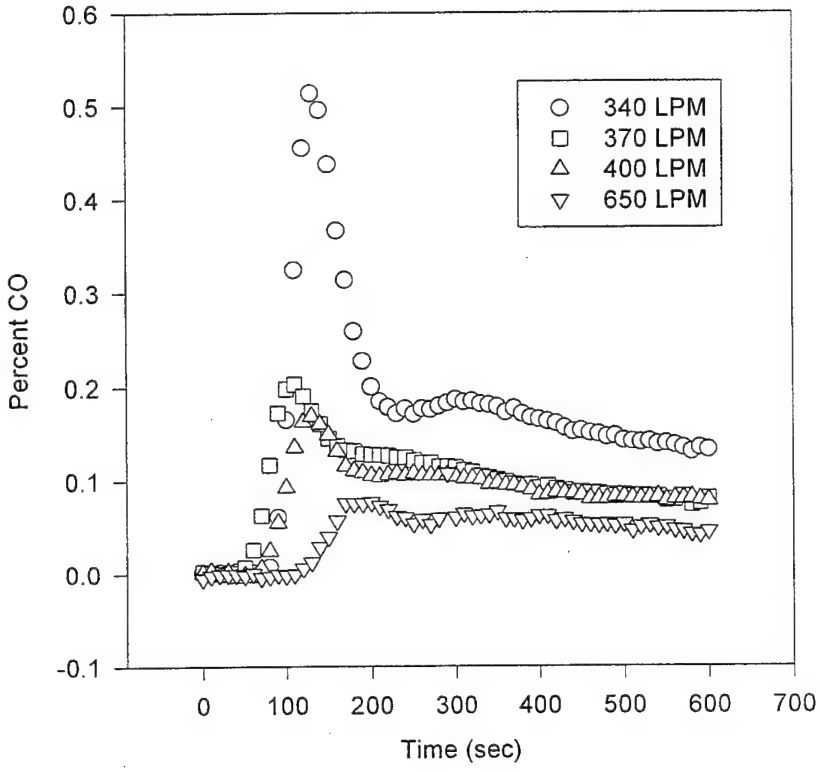

Figure 10. Carbon Monoxide production at 770 degrees C.

Maximal carbon monoxide concentrations were observed at approximately 100 seconds when evaluated at 770 degrees. Increasing the flow rate results in a decreased maximal concentration.

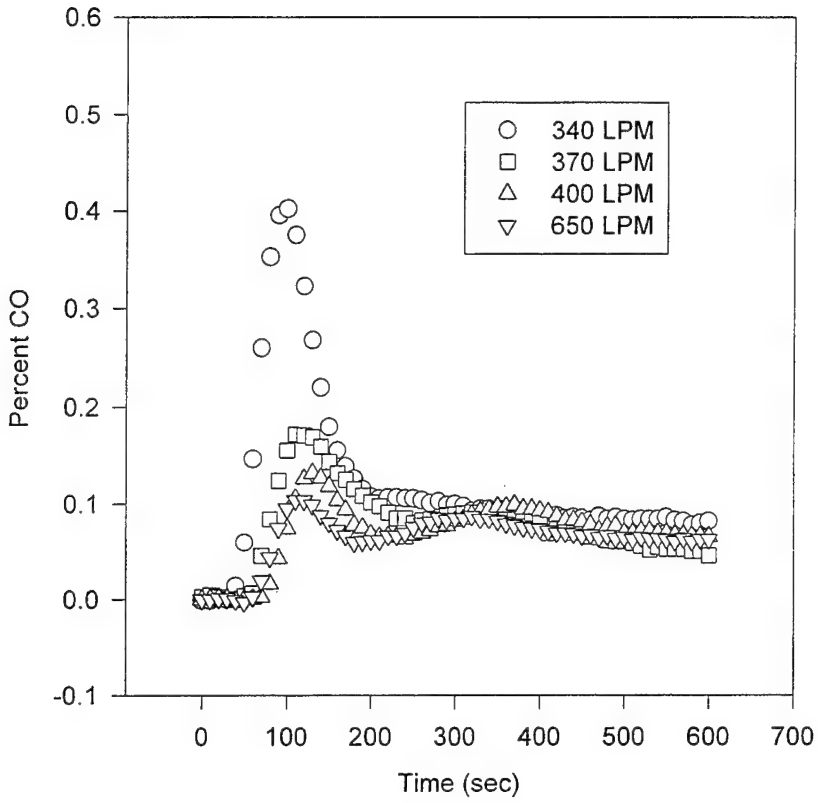

Figure 11. Carbon Monoxide production at 880 degrees C.

At 880 degrees, maximal carbon monoxide concentration was observed at approximately 90 seconds. Increasing the flow rate decreases maximal observed carbon monoxide.

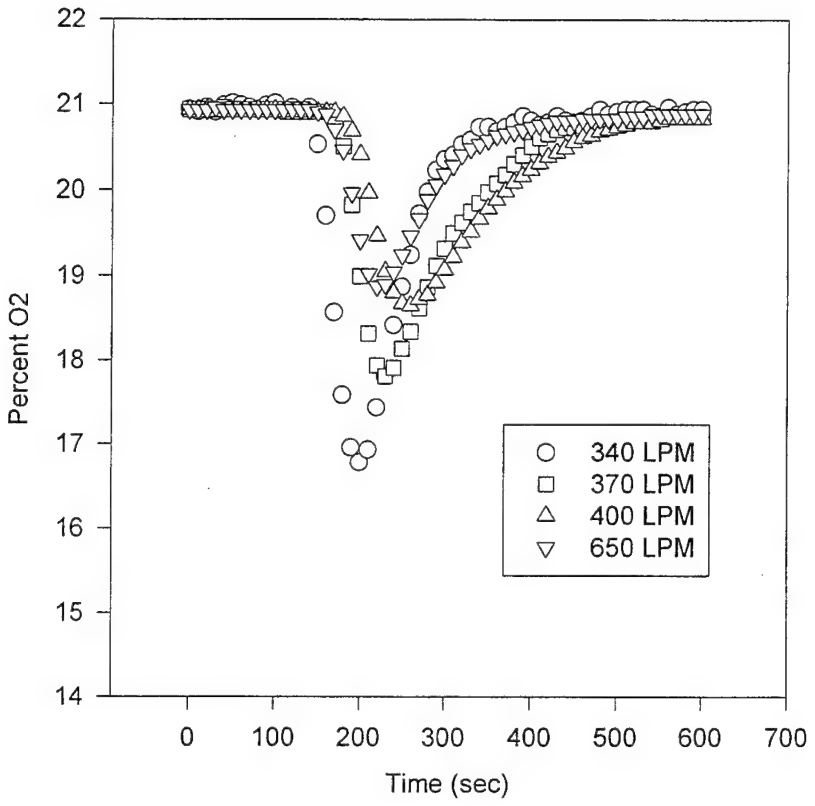

Figure 12. Oxygen depletion at 625 degrees C.

Oxygen was depleted to a minimum of approximately 14% under these conditions. Increasing the flow rate resulted in higher minimum concentrations of oxygen and a longer time required to produce the effect.

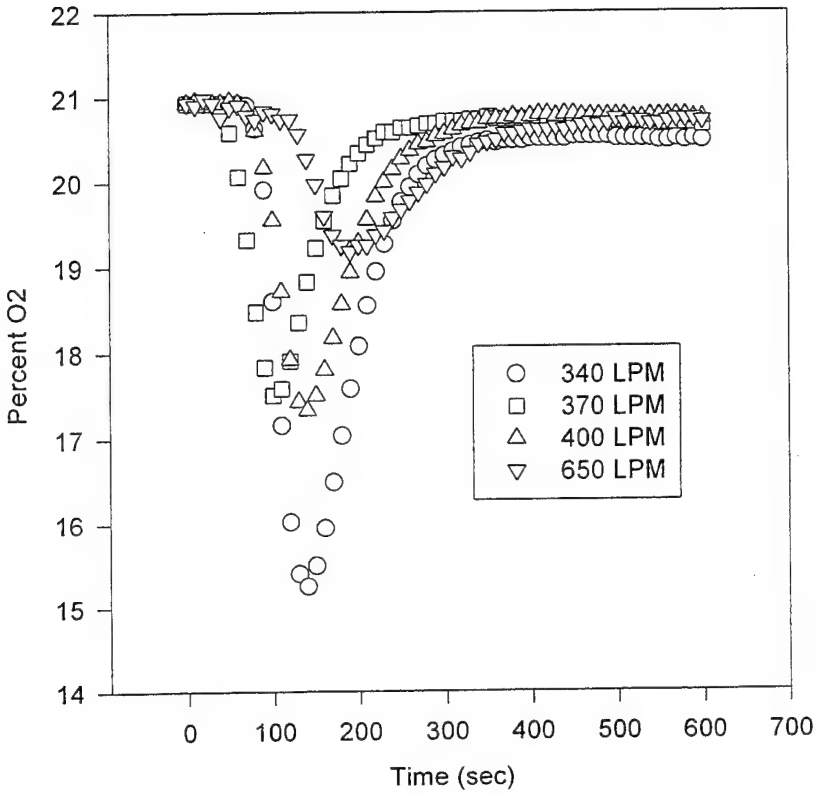

Figure 13. Oxygen depletion at 770 degrees C.

The depletion of oxygen at 770 degrees was observed to occur at approximately 125 seconds. Minimum oxygen concentrations of approximately 15% were observed at the lowest flow rate and the minimum oxygen concentration was higher at increased flow rates.

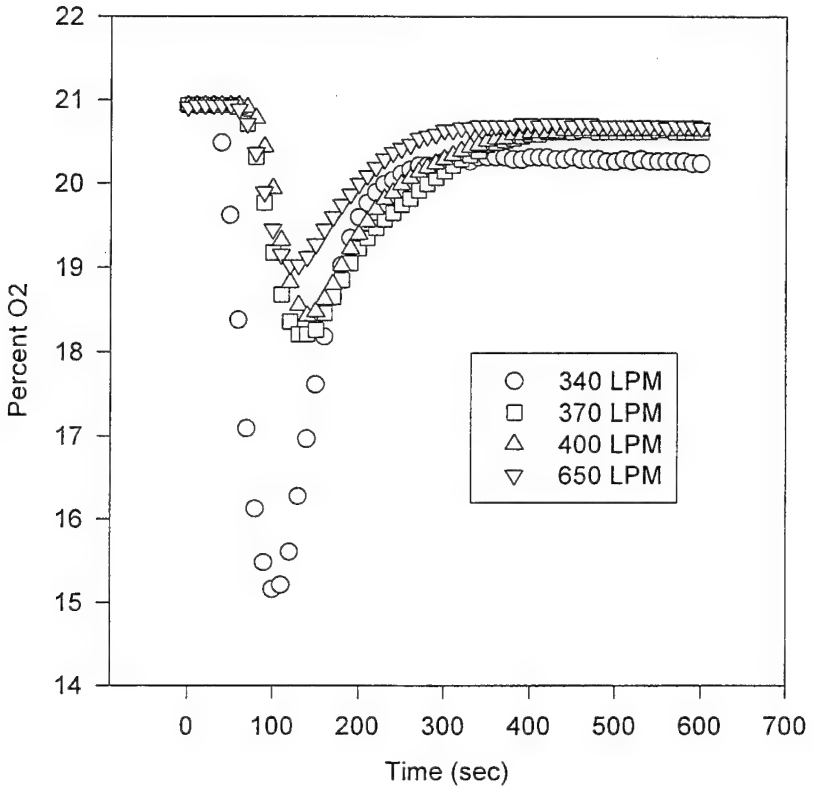

Figure 14. Oxygen depletion at 880 degrees C.

Maximal depletion of oxygen observed when combustion was accomplished at 880 degrees was observed at approximately 110 seconds. Oxygen was depleted to approximately 15%, roughly the same as in the 770 degree burn and two percent lower than in the 625 degree burn. Increasing the flow rate dramatically reduced the depletion of oxygen.

Particulate Analysis

Both temperature and flow influenced particle size (Table 5).

TABLE 5: MEAN DIAMETER (um) MEASUREMENTS OF SOOT PARTICLES FOR TEMPERATURE/FLOW RATE INTERACTIONS

TEMPERATURE	FLOW (L/min)	n	MEAN	SEM	MEDIAN	MODE(COUNT)
625	340	871	25.062	2.7599	11.333	11.333(35)
770	340	434	40.391	4.5433	15.333	14.000(25)
880	340	480	68.889	8.1756	13.333	0.288(30)
625	370	312	87.499	5.1251	68.055	0.388(10)
770	370	301	72.909	4.6786	36.667	0.381(24)
880	370	430	71.327	6.2665	15.278	0.192(17)
625	400	321	41.466	3.8755	0.962	0.286(29)
770	400	281	94.219	14.0865	17.778	0.291(14)
880	400	295	77.043	5.0191	38.889	0.291(26)
625	650	692	11.264	0.8065	6.547	0.291(70)
770	650	405	15.064	1.0751	13.333	11.333(23) 12.000(23)
880	650	499	10.767	1.4604	0.777	0.291(24)

At 770°C for a flow rate of 650 L/min, particle size significantly differed among the temperatures ($\chi^2 = 93.163$, df = 18, p = 0.0000). At a temperature of 770°C, the percent (26.4%) of particle size was less than one micron and the percent (68.9%) which was greater than ten microns were significantly different than the other temperatures (Table 6). At a temperature of 880°C, the percent (53.5%) of particle size which were less than one micron and the percent (39.5%) which were greater than ten microns were significantly different also. All three temperatures showed significant differences in particle size among the flow rates. See Table 7.

TABLE 6. THREE WAY INTERACTION FOR TEMPERATURE (°C)/FLOW (L/min)/INTERVAL(um)

TEMPERATURE	INTERVAL	COUNT	PERCENT	
FLOW 340				
625	0≤um≤1	329	37.8	3-Way Interaction
625	1<um ≤5	67	7.8	X^2 = 152.29
625	5<um ≤10	4	0.4	df = 54
625	10<um	471	54.1	p = 0.0000
770	0≤um≤1	84	19.4	
770	1<um≤5	12	2.8	
770	<um ≤10	2	0.2	
770	10<um	336	77.4	
880	0≤um≤1	162	33.8	
880	1<um≤5	32	6.7	
880	5<um≤10	3	0.6	
880	0<um	283	59.0	
FLOW 370				
625	0≤um≤1	94	30.1	
625	1<um≤5	27	8.6	
625	5<um≤10	5	1.5	
625	10<um	186	59.6	
770	0≤um≤1	93	30.9	
770	1<um≤5	31	10.3	
770	5<um≤10	1	0.3	
770	10<um	176	58.5	
880	0≤um≤1	166	38.6	
880	1<um≤5	35	8.2	
880	5<um≤10	7	1.6	
880	10<um	222	51.6	
FLOW 400				
625	0≤um≤1	161	50.2	
625	1<um≤5	48	14.9	
625	5<um≤10	3	0.9	
625	10<um	109	34.0	
770	0≤um≤1	93	33.1	
770	1<um≤5	29	10.3	
770	5<um≤10	8	2.9	
770	10<um	151	53.7	
880	0≤um≤1	93	31.5	
880	1<um≤5	29	9.9	
880	5<um≤10	2	0.6	
880	10<um	171	58.0	

TABLE 6 (Cont'd)

FLOW 650

625	0≤um≤1	306	44.2
625	1<um≤5	38	5.5
625	5<um≤10	3	0.4
625	10<um	345	49.9
770	0≤um≤1	107	26.4
770	1<um≤5	18	4.4
770	5<um≤10	1	0.2
770	10<um	279	68.9
880	0≤um≤1	267	53.5
880	1<um≤5	31	6.2
880	5<um≤10	4	0.8
880	10<um	197	39.5

TABLE 7. CHI-SQUARED DIFFERENCES IN FLOW RATE FOR EACH TEMPERATURE

TEMPERATURE	CHI-SQUARED	D.F.	PROB.
625	92.048	30	0.0000
770	96.771	30	0.0000
880	96.425	30	0.0000

At 770°C, the percent of particles which was greater than 50% of all flow rates. A flow rate of 340 L/min had a significantly higher percent (77.4%) above 10 microns and a significantly lower percent (19.4%) of particle size less than one micron. For 880°C, 53.5% of the particles were less than one micron which was significantly higher than the other flow rates. At 880 °C and 650 L/min had the greatest particles less than one micron. At 770°C and 340 L/min had the highest number of particles greater than 10 microns. Scanning electron micrographs (Figures 15-17) show amorphous particles of various sizes, specifically the respirable portions, at both the closest (10 ft) and furthest (40 ft) sections of the tunnel.

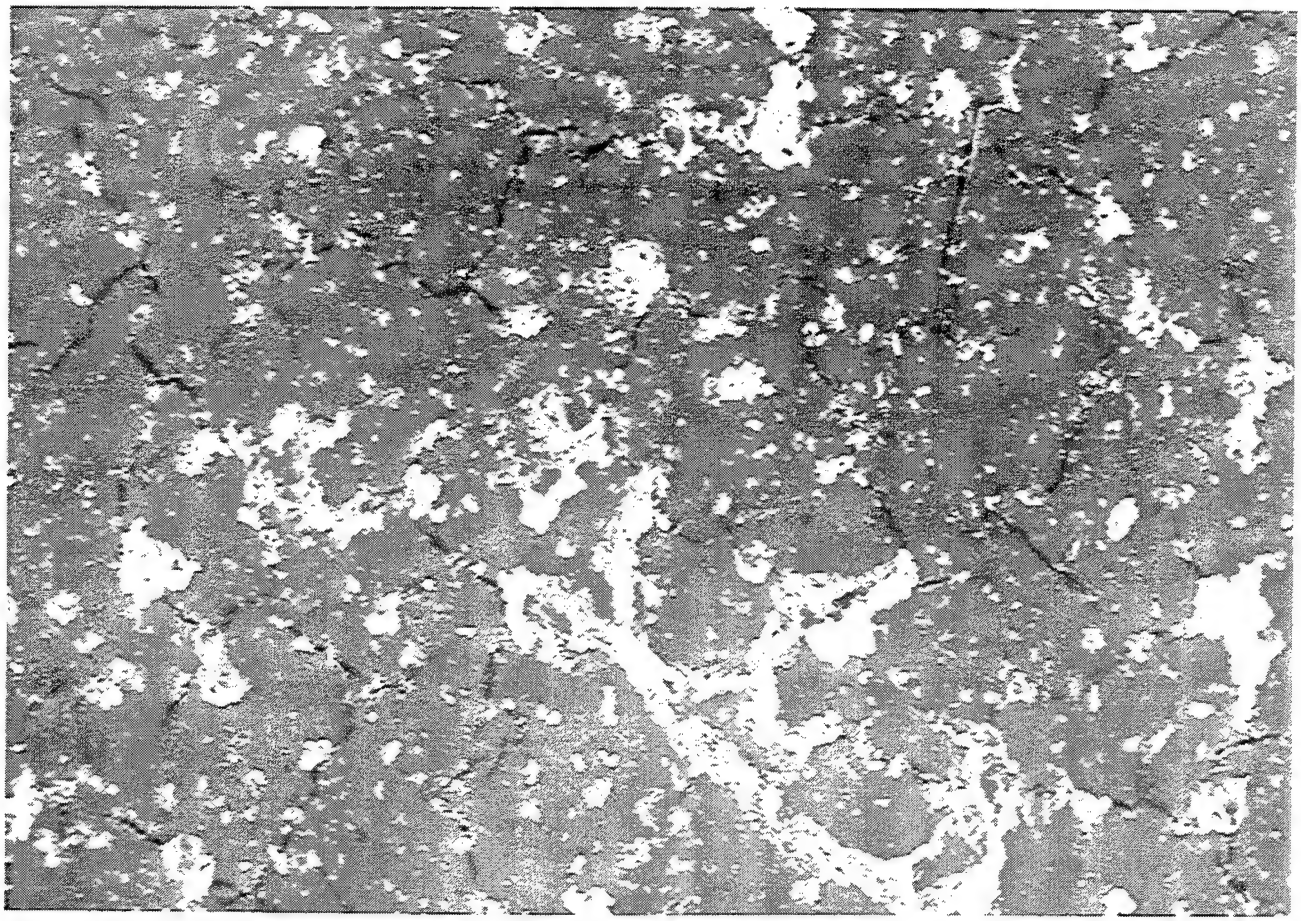

Figure 15. Electron Photomicrograph of Particulate Matter, (30x, 10 feet Downstream). Gravity deposition of particles from ACM combustion at 625° C., 340L/min. ventilation pressure at sampling port 1 (approximately 10 ft. from the furnace). Low magification micrograph showing large "clumps"of material and distribution of smaller particles. Accelerating Voltage = 20kV.

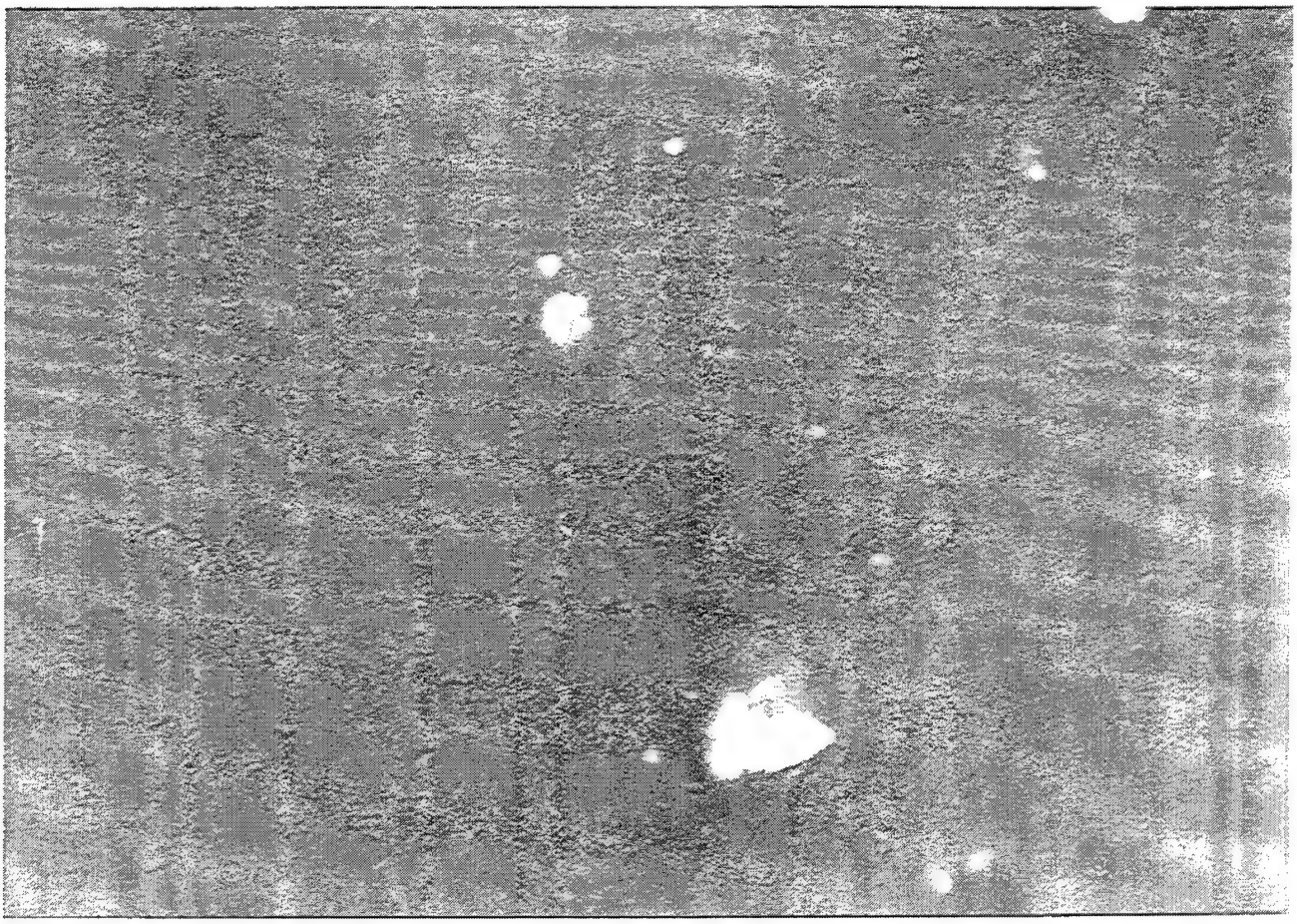

Figure 16. Electron Photomicrograph of Particulate Matter, (15,000x, 10 feet Downstream). Gravity deposition of particles from ACM combustion at 625° C., 340L/min. ventilation pressure at sampling port 1 (approximately 10 ft. from the furnace). High magnification scanning electron micrograph showing relative abondance and detail of respirable particles (< 1um). Accelerating voltage = 20kV.

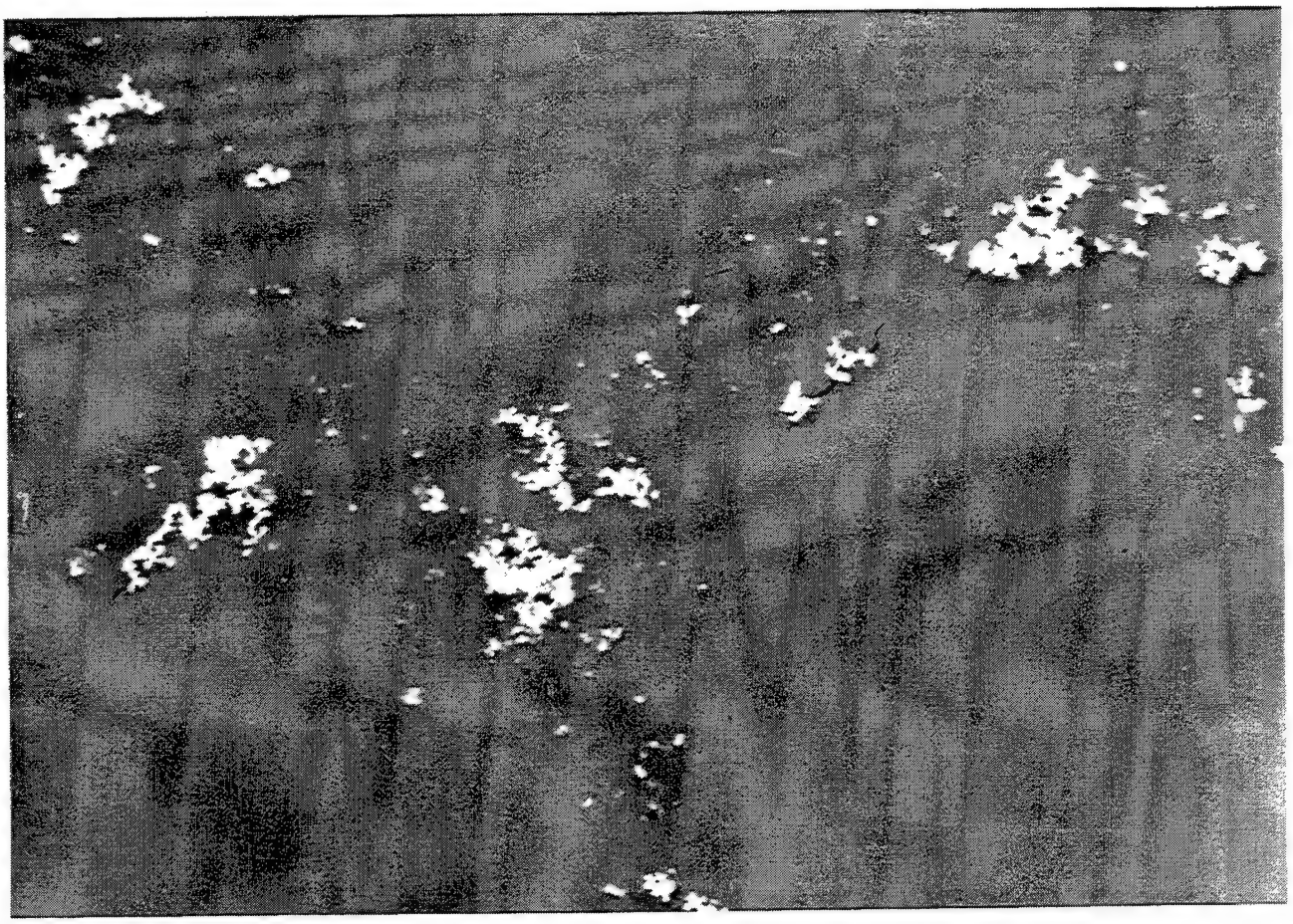

Figure 17. Electron Photomicrograph of Particulate Matter, (4,500x, 10 feet Downstream). Gravity deposition of particles from ACM combustion at 625° C., 400L/min. air flow at sampling port 4 (approximately 40 ft. from the furnace). Micrograph reveals detail of ACM particles. Note the abundance of small particles, which are respirable (< I um). Accelerating voltage = 20kV.

DISCUSSION

In the present assessment we have evaluated the combustion-induced disposition of a form of ACM which is intended for use in advanced aircraft. The goal of this study was to obtain a qualitative listing of compounds produced from combustion of ACM. As such, we focused on three areas: A) that material which remained behind following combustion, B) the volatile compounds which were released following combustion, and C) the nature of any particulate material released through combustion. Our data revealed that the majority (50-75%) of the actual ACM remained behind following combustion as a carbon-fiber based material. This presumably represents the fibers which are embedded in the epoxy binder of the composite. The human health threat of the remaining material still remains to be characterized.

The balance of the material was combusted to CO, CO_2, water and other material-specific products of combustion. These materials underwent further analysis: 1) vapors produced were trapped in solvent and analyzed by gas chromatography, 2) particulate matter (solid phase soot deposited on filters and plates) was characterized for particle size distribution and extracted with solvent to determine chemical composition. These analyses have identified nearly 90 chemicals produced from the combustion of ACM. The solid (soot) phase was deposited along and at the end of the furnace vent tube. While the intent of this investigation was to determine qualitatively the types of compounds which result from ACM combustion, some quantitation of ACM disposition has been attempted. Subtracting the mass of material remaining in the calorimeter from the starting mass, we have shown that approximately 30% of the starting mass is vented during combustion. The mass loss rate was previously found to be useful for scaling up from laboratory data and permits modeling the resultant smoke and aerosol plume. The initial analysis of data collected from cascade impactor samples show that approximately 50% of the particles in the smoke have an aerodynamic diameter less than 10 microns (10um). The implication of this finding is that the inhalation hazard may be substantial for the combustion products of ACM, given the complex organic composition of the smoke and the small particle size. Particles less than 1.0 um have the potential for deposition within the alveoli of the lungs, the site of oxygen absorption. We have clearly identified chemical products of ACM on these particles. The presence of these potentially dangerous chemicals with particulate matter raises the probability of deposition of these chemicals within the alveoli. This may result in increased potential for toxic consequences.

Soot (Table 1) and vapor (Table 2) were analyzed for compound identification by mass spectroscopy using spectra library but not confirmed by chemical standards. Of the volatiles trapped in solvent and analyzed by gas chromatography, it appears that eight major constituents can account for 90+% of the volatiles. Of the soot recovered, approximately 30% of the mass was extractable and identifiable by gas chromatography (routine method of analysis). The results of this examination identified over 80 individual compounds. The fourteen major compounds from this analysis accounted for less than 3% of the soot mass. Subjective analysis of the soot revealed a fine, black amorphous powder which packed loosely (1.5 grams occupied 5 ml, where 1.5 grams water would occupy 1.5 ml) and was consistent with elemental carbon.

Known toxicology exists on only a few of the major compounds identified above. This preliminary study identified three main classes of combustion products: nitrogenous aromatic compounds, PAHs and phenols.

ANILINE - Effects include: methemoglobinemia (Amdur et al, 1993).

2 AND 3-METHYLANILINE - Commonly known as Toluidine. There is epidemiological evidence that associates occupational exposures to an increase risk of bladder cancer and related to duration of exposure. There is inadequate evidence of carcinogenicity in humans but sufficient evidence in animals. Therefore it is considered a possible carcinogen to humans. Vapor toxicity is much like aniline with less effect on CNS and more on vascular. Toxicity and biomedical effects include: CNS depression, cyanosis, methemoglobinemia, vertigo, headache, and mental confusion (NIOSH, 1990, Hamilton and Hardy, 1974, and Budavari, 1989).

QUINOLINE - It is known to have liver cancer activity in mice and is mutagenic. Exposure may affect cardiovascular system, CNS, retina, and optic nerve. Quinoline is found in tobacco smoke as well as particulates in urban air. If released to the atmosphere, the vapor is expected to react with hydroxyl radicals with an estimated half-life of 2.5 days (Clayton, 1981 and Amdur et al, 1993).

1,2-DIHYDRO-2,2,4-TRIMETHYLQUINOLINE - Negative for mutagenicity. Similar effects as quinoline (Zeiger, 1987).

ANTHRACENE - In itself is not carcinogenic, however many of its derivatives found as combustion by-products are potent carcinogens. They are commonly found in coal tar, tobacco smoke and petroleum products. Acute toxicity is presumably due mostly to derivatives and may cause an excess of bronchitis (USEPA IRIS, 1994, Clayton, 1981 and Amdur et al, 1993).

FLUROANTHENE - Commonly released into the environment from general use in combustion of organic matter, fossil fuels, smoking and charcoal broiling as to generate PAHs. Unabsorbed chemical in air will photolyze with a half-life approximately 4-5 days. Effects from exposure may include nausea, tachycardia, cardiac arrhythmia's, liver injury, pulmonary edema, and respiratory arrest. NIOSH recommends it be regulated as an occupational carcinogen, however; it is not classified as a human or animal carcinogen (USEPA IRIS, 1994, IARC, 1987, and USEPA, 1980).

DIPHENYL ETHER - Not a serious hazard or mutagenic. Diphenyl ether is reportedly released from combustion emissions of plastic manufacturing and turbine engines. It is used in various soaps, detergents and as a dye carrier in textile operations. Acute oral exposures in rats have shown injury to liver, spleen, kidney, thyroid and intestinal tract (Clayton, 1981 and Graedel, 1986).

DIBENZOFURAN - Not considered carcinogenic for either human or animal but has been associated with chloracne as has a number of other chlorinated aromatic compounds. It is a common emission associated with combustion of coal and fuel. In the gas phase it will degrade rapidly (half-life of approximately 11 hours) and as a particulate may be relatively persistent (USEPA IRIS, 1994 and Amdur et al, 1993).

N-HYDROXYMETHYLCARBAZOLE - Shown to have mutagenic activity (Ibe and Raj, 1994).

PHENOL - Observed effects from acute exposure may include: shock, hypotension, methemoglobinemia, Heinz body hemolytic anemia pulmonary edema, dark urine, and death due to action on CNS, cardiovascular system, lung and kidney. Primary site of action is CNS. Phenol is not classified as carcinogenic to humans (Amdur et al, 1993 and Gosselin et al, 1984).

It is important to compare the implications of toxicity from this limited-scope evaluation of ACM combustion to the scenario involving the complete aircraft. As with any exposure to burning materials, proximity correlates well with toxicity. The use of PPE equipment may abate the dangers associated with products of combustion, but PPE may not be available to all exposed personnel.

This project has evaluated the combustion-related chemical release from an ACM destined for use in structural components of advanced aircraft. The results of this study have established the expected products of combustion from this specific ACM matrix. Modifying matrix components will result in altered combustion products, and the potential interaction between combustion products of specific matrix components may also change the pattern of compounds ultimately released by combustion. While the use of ACM in aircraft in development is increasing steadily, ACM presently accounts for less than half the total mass of the most advanced aircraft. In the event of a mishap, the entire airframe may be subjected to combustion. The products released from the combustion of rubber, plastic, fuel, lubricants and hydraulic fluids and insulation should be considered in any assessment of toxicity risk from a burning aircraft.

RECOMMENDATIONS

We recommend a quantitative analysis of the volatiles released and a thorough evaluation of the deposited soot to include high performance liquid chromatography-mass spectrometry and secondary confirmation, such as Infra-Red spectroscopy. We will continue to evaluate data in hand to determine if a preliminary estimate of the quantity of volatiles released can be obtained.

Because the quantity of volatiles combined with soot accounts for approximately 35% of the total material, and because such a high percentage of the volatiles are accounted for in the eight identified compounds, we highly recommend the further analysis of deposited soot. A specific analysis for carbon content would yield valuable data, as our subjective reports implicate elemental carbon as a major constituent of soot.

A quantitative evaluation of carbon dioxide, carbon monoxide and water produced will reduce the quantity of ACM not specifically accounted for. Hydrogen cyanide is an additional combustion product which should be quantitated. It is commonly produced with nitrogenous products. Even a precise estimation of total soot produced would strengthen the recovery information.

Due to the large percentage of respirable particles and the complexity of the organic mixture associated with those particles, bioassay is necessary to determine physiological and pathological outcomes. (Levin et al, 1987).

Cascade impactors can be used to determine particle size distribution of an air sample. A series of impingement plates can collect particles in different size ranges thus allowing investigators to analysis for total weight, particle count and chemical composition.

REFERENCES

Amudr, M.O., J. Doull, C.D. Klaassen (eds.). Casarett and Doul's Toxicology The Basic Science of Poisons. 4th ed. New York: McGraw-Hill Inc., 1993.

Babrauskas, V., B.C. Levin, and R.G. Gann. 1987. "A new approach to fire toxicity data for hazard evaluation", Fire Journal, March/April: 22-28 and 70-71.

Budavari, S. (ed.). The Merck Index - Encyclopedia of Chemicals, Drugs and Biologicals. Rahway, NJ: Merck and Co., Inc., 1989.

Caldwell, D.J. and Y. Alarie. 1990a. A method to determine the potential toxicity of smoke from burning polymers:I. Experiments with Douglas fir., J. of Fire Sciences, 8:23-62

Caldwell, D.J. and Y. Alarie. 1990b. A method to determine the potential toxicity of smoke from burning polymers:II. The toxicity of smoke from Douglas Fir., J. of Fire Sciences, 8:275-309.

Caldwell, D.J. and Y. Alarie. 1991. A method to determine the potential toxicity of smoke from burning polymers:III. Comparison of synthetic polymers to Douglas fir using the UPITT II flaming combustion/toxicity of smoke apparatus, J. of Fire Sciences, 9:470-518.

Caldwell, D.J., K.J. Kuhlmann, and J.A. Roop. 1995. "Smoke Production From Advanced Composite Materials", in: Fire and Polymers II: Materials and Tests for Hazard Prevention, ACS Symposium Series 599, American Chemical Society, Washington, DC.

Clayton, G.D. and F.E. Clayton (eds.).Patty's Industrial Hygiene and Toxicology: Volume 2A, 2B, 2C: Toxicology. 3rd ed. New York: John Wiley Sons, 1981-1982.

Gosselin, R.E., R.P. Smith, H.C. Hodge. Clinical Toxicology of Commercial Products. 5th ed. Baltimore: Williams and Wilkins, 1984.

Graedel, T.E.. Atmospheric Chemical Compounds. Orlando, FL: Academic Press Inc, 1986.

Hamilton, A. and H.L. Hardy. Industrial Toxicology. 3rd ed. Acton, MA: Publishing Sciences Group, Inc., 1974.

Hochberg, Y. and A.C. Tamhane. 1987. Multiple Comparison Procedures. New York: John Wiley & Sons.

IARC. Monographs on the Evaluation of the Carcinogenic Risk of Chemicals to Man. Geneva: World Health Organization, International Agency for Research on Cancer, 1972-PRESENT. (1987).

Ibe, B.O. and J.U.Raj. 1994. "Metabolism of N-methylcarbazole by rat lung microsomes", Exp. Lung Res., May-Jun; 20(3), 207-22.

Levene, H. 1960. "Robust tests for equality of variance", In Contributions to Probability and Statistics, ed. I. Olkin. Palo Alto: Stanford University Press.

Levin, B., M. Paabo, J.L. Gurman and S. E. Harris. 1987. "Effects of exposure to single or multiple combinations of the predominant toxic gases and low oxygen atmospheres produced in fires", Fund. Appl. Tox, **9**:236-250.

Miller, C.R., J.H. Grabau, K.J. Kuhlmann, J.W. Lane, M.J. Walsh, and D.J. Caldwell. 1995. "Combustion products of Advanced Composite Materials (ACM): Evolution of the UPITT II method", Toxicologist 15.

NIOSH; NIOSH Alert: Preventing Bladder Cancer form Exposure to o-Toluidine and Aniline (1990).

Ohlemiller, T., T. Cleary, J. Brown, and J. Shields. 1993. "Assessing the Flammability of Composite Materials", J. of Fire Sciences, **2**:308-319.

Roop, J.A., D.J. Caldwell, and K.J. Kuhlmann. 1994. "Modeling Aerosol Emissions from the Combustion of Composite Materials", in: Environmental, Safety, and Health Considerations - Composite Materials in the Aerospace Industry, NASA Conference Publication 3289, National Aeronautics and Space Administration, Greenbelt, MD.

Royston, J.B. 1982. "An extension of Shapiro and Wilk W test for normality to large samples", Applied Statistics, 31:115-124.

Shapiro, S.S. and M.B. Wilk. 1961. "An analysis of variance test for normality", Biometrika, 52:591-611.

USEPA; Ambient Water Quality Criteria Doc: Polynuclear Aromatic Hydrocarbons 1980.

USEPA's Integrated Risk Information (IRIS) from MedLine Express, 1996.

Winer, B.J. 1971. STATISTICAL PRINCIPLES IN EXPERIMENTAL DESIGN,2nd edition. New York: McGraw-Hill Book Company.

Zeiger E.. Environ Mutagen 9:1-110 (1987) (cited in HSDB July 1995).

APPENDIX A

Appendix A: GC/MS Conditions

Set Points

Oven Temp 1	35.0	Oven Temp 3	300.0
Oven Time 1	5.0	Oven Time 3	20.0
Oven Rate 1	3.0	Oven Rate 3	0.0
Valve 1		Off Valve 3	NONE
Oven Temp 2	120.0	Oven Temp 4	0.0
Oven Time 2	20.0	Oven Time 4	0.0
Oven Rate 2	3.0		
Valve 2		NONE Valve 4	NONE
Aux. Zone	220.0	Inj. Temp 1	270.0
Pressure 1	13.0	Inj. Temp 2	NONE
Pressure 2	0.0		

Timed Events

	Time	Event	Value
1	-0.10	V1	Off
2	1.00	V1	On
3	...		

MS Parameters

Starting Mass	35
Ending Mass	650
Multiplier HV	1725 (for instrument)
Runtime (min)	170
Filament delay (sec)	270

APPENDIX B

Appendix B. Approximate Quantification of Identified Compounds Found in Soot

Compound	Soot. Conc. ug/g	Soot. Conc. % weight
2-Hydroxybenzonitrile	214	0.02%
Aniline	2990	0.30%
Phenol	2170	0.22%
3-Methylphenol	46.1	0.00%
3-Methyl-1-isocyanobenzene	2.7	0.00%
1,2-Methylphenol	55.5	0.01%
3-Methylaniline	626	0.06%
2-Methylaniline	578	0.06%
4-Methylphenol	160	0.02%
4-Methylaniline	11.7	0.00%
2-Methylphenol	206	0.02%
4-Methyl-1-isocyanobenzene	15.2	0.00%
N-(1-Phenylethylidene)-methanamine	25.2	0.00%
Naphthalene	256	0.03%
4-Aminostyrene	13.4	0.00%
Quinoline	3480	0.35%
Isoquinoline	186	0.02%
2-Aminoisocyanate	39.3	0.00%
1-Methylnaphthalene	33.2	0.00%
2-Methylnaphthalene	33.2	0.00%
Indole	537	0.05%
2-Propenenitrile,3-phenyl-, (E)-	40.5	0.00%
1-Methylisoquinoline	236	0.02%
8-Methylquinoline	260	0.03%
5-Methylquinoline	1200	0.12%
3-Methylquinoline	353	0.04%
7-Methylisoquinoline	141	0.01%
2-Aminobenzonitrile	354	0.04%
3-Methylisoquinoline	201	0.02%
2-Ethenylnaphthalene	529	0.05%
N-Phenylacetamide	156	0.02%
1-Naphthalenemethylphenylacetate	152	0.02%
5-Methylindolizine	121	0.01%
Diphenylether	1050	0.11%
4,8-Dimethylquinoline	12.0	0.00%
5,8-Dimethylquinoline	2.4	0.00%
Benzene, (2,4-cyclopentadien-1-ylidene)me	3.2	0.00%
Diphenylmethane	0.9	0.00%
2-Methoxyethoxybenzene	1660	0.17%
1,2-Dihydro-2,2,4-trimethylquinoline	2210	0.22%
4,8-Dimethylisoquinoline	56.5	0.01%
2-Phenylpyridine	408	0.04%

1-Methyl-4-phenylpyridinium	132	0.01%
4,8-Dimethylquinoline]	1.8	0.00%
1,2-Dihydrocyclobuta[b]quinoline	38.9	0.00%
2-Isocyanonaphthalene	2210	0.22%
4-Methyl-1,1'-biphenyl	19.6	0.00%
Dibenzofuran	1360	0.14%
1-Isocyanonaphthalene	1660	0.17%
1,2,4,6-Tetramethyl-1,4-dihydropyridine-	629	0.06%
2,4,4,6-Tetramethyl-1,4-dihydropyridine-	212	0.02%
Fluorene	584	0.06%
1-Isocyanatonaphthalene	165	0.02%
5-Methylpyrimido[3,4-a]indole	2.8	0.00%
1H-Phenaline	71.1	0.01%
1,1-Diphenylhydrazine	285	0.03%
5H-Indeno[1,2-b]pyridine	87.6	0.01%
2-(Phenylethynyl)pyridine	103	0.01%
1,1'-Biphenyl-2-carbonitrile	130	0.01%
2-Methyl-N-phenylaniline	30.7	0.00%
1,1-Diphenylhydrazine	110	0.01%
Dibenzothiophene	280	0.03%
Anthracene	1700	0.17%
Phenanthrene	521	0.05%
4(1H)-Pteridinone, 2-amino-7-methyl-	286	0.03%
9-Methylacridine	48.9	0.00%
9H-Fluoren-9-imine	352	0.04%
N-Hydroxymethylcarbazole	1290	0.13%
1-(Phenylmethylene)-1H-indene	81.6	0.01%
2-Phenylnaphthalene	238	0.02%
4-Phenylisoquinoline	64.0	0.01%
8-Phenylisoquinoline	128	0.01%
Fluoranthene	1300	0.13%
9-Methoxyanthracene	153	0.02%
9-Phenanthrenecarboxaldehyde, O-acetylox	117	0.01%
Pyrene	701	0.07%
5-Benzoquinoline	98.3	0.01%
Indeno(1,2,3-ij)isoquinoline	564	0.06%
Fluoranthene	832	0.08%
2,4-Imidazolidinedione, 1,3,5-trimethyl-	258	0.03%
Acenaphtho(1,3-B)pyridine	217	0.02%
Phenanthrene, 4-ethyl-5-methyl	124	0.01%
7H-Benzo[c]fluorene	160	0.02%
Benz[a]anthracene, 1,2,3,4,7,13-hexahydr	197	0.02%
Naphthacene	123	0.01%
Chrysene	362	0.04%
Benzo[e]pyrene	550	0.06%
Benzo[j]fluoranthene	205	0.02%

9,10,11,12-Tetrahydrobenzo[e]pyrene	183	0.02%
Benz[e]acenaphthrylene	228	0.02%